SAGE-Hindawi Access to Research
International Journal of Electrochemistry
Volume 2011, Article ID 692603, 6 pages
doi:10.4061/2011/692603

Research Article

Preparation and Capacitive Behavior of Dandelion-Like γ-MnO_2 Nanofibre/Activated Carbon Microbeads Composite for the Application of Supercapacitor

Li Bai, Xianyou Wang, Xingyan Wang, Xiaoyan Zhang, Wanmei Long, Hong Wang, and Jiaojiao Li

Key Laboratory of Environmentally Friendly Chemistry and Applications of Ministry of Education, School of Chemistry, Xiangtan University, Hunan, Xiangtan 411105, China

Correspondence should be addressed to Xianyou Wang, wxianyou@yahoo.com

Received 12 April 2011; Accepted 23 July 2011

Academic Editor: Yuping Wu

Dandelion-like γ-manganese dioxide (γ-MnO_2) nanofibre/activated carbon microbeads (ACMBs) composite is prepared by an in situ coating technique. The structure and morphology of the composite are characterized by scanning electron microscopy and X-ray diffraction. The results show that γ-MnO_2 nanofibre is uniformly encapsulated on the surface of ACMB, and the composite finally becomes a dandelion-like microbead. Cyclic voltammetry, galvanostatic current charge/discharge, and cycle life measurements are used to evaluate the electrochemical behaviors of the composite. Since the composite is able to undergo pseudofaradic charge transfer reactions and hereto contributes together with the double-layer effect to the total capacitance of the material, the specific capacitance of the composite is as high as 375.9 F g^{-1} at a scan rate of 1 mV s^{-1}, which is significantly higher than the pure ACMB. Besides, the capacitance retention of the supercapacitor using the composite as electrode-active material keeps still 93% after 1000 cycles.

1. Introduction

Currently, electrochemical supercapacitors are extensively studied as auxiliary energy storage devices to be used with rechargeable batteries. Their applications include electric vehicles, renewable energy, mobile generator devices, direct-current power systems, and uninterruptible power supplies [1]. On the basis of the energy storage mechanism, supercapacitors can be classified into two categories [2], namely the electrical double-layer capacitor and the faradic pseudocapacitor. The capacitance of the former comes from the charge accumulation at the electrode/electrolyte interface, therefore, strongly depending on the surface area of the electrode accessible to the electrolyte. The capacitance of the latter is due to the reversible faradic redox reaction of electroactive species on the electrode, such as surface functional groups and transition metallic oxides. It is obvious that the electrode takes the important part in the development of supercapacitors.

Carbon microbeads have several advantages, such as high electrical conductivity, good fluidity, excellent sphericity, easy-to-control pore size distribution and a relatively low cost [3]. Usually, the carbon materials only possess double-layer capacitance, while metallic oxide possesses faradic pseudocapacitance, and the faradic pseudocapacitance is almost 10–100 times higher than double-layer capacitance [4]. Transition metallic oxides have been widely studied as promising materials for electrochemical capacitors due to their redox chemistry, large pseudocapacitance, and high power and energy density.

An improvement in the capacitance of carbon material can be realized by preparing carbon/metallic oxide composites. Recently, many carbon/transition metallic oxides or hydroxide composites for the application of supercapacitor have been widely developed, which are based on a combination of double-layer capacitance and faradic pseudocapacitance [5–8]. With regard to metallic oxides, amorphous hydrated ruthenium oxide has been found

to be an excellent electrode [9, 10] because of its ideal pseudocapacitance behavior (as high as 760 F g^{-1} specific capacitance) and good reversibility. However, the high cost of this precious metallic oxide hinders its practical application. Hence, seeking for inexpensive metallic oxides, for example, NiO, CoO_x, SnO_2, Mn_3O_4, and MnO_2, as alternative electrode materials is of great interest [11–16]. With its low cost and environmental friendliness, the manganese oxides with various crystal structures have been intensively investigated as electrode-active materials of supercapacitor [17, 18].

It has been found that appropriate MnO_2 modification on the surface of carbon material can apparently improve its capacitive behavior. It has been reported that the specific capacitance of the carbon aerogel loaded with MnO_2 can increase from 133 F g^{-1} to 219 F g^{-1} [19]. Our group prepared the MnO_2/carbon aerogel composite by chemical co-precipitation and obtained a high specific capacitance of 226.3 F g^{-1} [5].

Although some works have been carried out on composites of activated carbon, CNTs, carbon aerogel, and carbon fiber coated with MnO_2, there is less reported on γ-MnO_2 nanofibre/ACMB composite. In this paper, dandelion-like γ-MnO_2 nanofibre/ACMB composites were prepared by an in situ coating technique. The electrochemical performances of γ-MnO_2 nanofibre/ACMB composite were investigated in detail.

2. Experimental

2.1. Preparation of γ-MnO_2 Nanofibre/ACMB Composite Electrode. All chemical reagents were the analytical grade and directly used as received. ACMB was prepared by a typical hydrothermal technique as follow. The glucose (1.5 mol L^{-1}) was put into a Teflon-lined stainless steel autoclave of 100 mL capacity. The autoclave was sealed and maintained at 160°C for 18 h in an oven, then cooled to room temperature naturally. A brown precipitate was collected, washed with distilled water and absolute ethanol. Then the obtained sample was dried in a vacuum oven at 80°C for 12 h. Finally, the sample was carbonized at desired temperature 750°C for 1 h in a flow of Ar, followed by concentrated nitric acid activation at 70°C stirred for 24 h to form ACMB.

The in situ preparation process of γ-MnO_2 nanofibre/ACMB composite was as follow: firstly, 1.0 g ACMB was dispersed in 150 mL of distilled water by ultrasonic vibration for 10 min. Secondly, 1.9441 g $MnSO_4 \cdot H_2O$ was added into the above suspension, and stirred for 30 min at room temperature. Subsequently, 3.1106 g $K_2S_2O_8$ was added into the above solution according to chemical stoichiometric ratio, and then refluxed 6 h at 100°C under an uninterrupted stir. The resulting γ-MnO_2 nanofibre/ACMB composite precipitate was filtered and washed with distilled water and ethanol several times until the filtrate was about neutrality. Then the product was dried at 80°C for 8 h in an oven. Finally, γ-MnO_2 nanofibre/ACMB composite was obtained. The content of γ-MnO_2 nanofibre in the dandelion-like γ-MnO_2 nanofibre/ACMB composite was about 20 wt.%.

2.2. Measurement Techniques of Structural Characterization..

(i) Scanning electron microscopy (SEM) (JSM-6610, JEOL) was used to study the morphology and surface structure of the samples.

(ii) X-ray diffraction (XRD) of samples was performed on a diffractometer (D/MAX-3C) with Cu Ka radiation (λ = 1.54056 Å) and a graphite monochromator at 50 kV, 100 mA.

2.3. Evaluation of Electrochemical Properties. The mixture containing 80 wt.% γ-MnO_2 nanofibre/ACMB, 10 wt.% acetylene black and 10 wt.% polyvinylidene fluoride (PVDF) was well mixed in N-methyl-2-pyrrolidone (NMP) until to form the slurry with proper viscosity, and then the slurry was uniformly laid on a Ni foam that was used as a current collector (area was about 1.5 cm^2) and then dried at 80°C for 12 h. The Ni foam coating γ-MnO_2 nanofibre/ACMB composite was pressed for 1 min under a pressure of 1.6×10^6 Pa. The electrochemical performances of the prepared electrodes were characterized by cyclic voltammetry (CV) and charge/discharge tests. The used electrolyte was 6 mol L^{-1} KOH solution. The experiments were carried out using a three-electrode cell, in which the Ni foam and the saturated calomel electrode were used as counter and reference electrodes, respectively. The cyclic voltammetry and the charge/discharge measurements at constant current were performed by means of electrochemical analyzer systems, CHI660 (CH Instruments, USA). The cycle life was carried out by potentiostat/galvanostat (BTS6.0, Neware, Guangdong, China) on button cell supercapacitors, and the symmetrical button cell supercapacitors were assembled according to the order of electrode-separator electrode

3. Results and Discussion

3.1. Material Characterization. Figure 1 presents the SEM images of the ACMB and γ-MnO_2 nanofibre/ACMB composite. As being seen from Figure 1(a), the carbon microbeads are good dispersity, smooth surface, perfect spherical morphology, and about 2 μm average size. The images in Figures 1(b) and 1(c) show that the γ-MnO_2 nanofibre/ACMB composite keeps the spherical morphology of ACMB, but the surface of the ACMB sphere is covered by a lot of γ-MnO_2 nanofibers and finally becomes a dandelion-like appearance. The average diameter of the dandelion-like γ-MnO_2 nanofibre/ACMB composite is about 3 to 4 μm. The dandelion-like appearance of the γ-MnO_2 nanofibre/ACMB composite can provide not only bigger specific surface area, but also higher electron and ion conductivity as electrode-active material of supercapacitor. Besides, γ-MnO_2 nanofibre can also play an important role as a pathway of electron transfer continuously and electrolyte conveyance during charging/discharging process for supercapacitor.

Figure 2 shows XRD patterns of (a) ACMB and (b) γ-MnO_2 nanofibre/ACMB composite. In Figure 2(a), the XRD pattern of ACMB reveals the broad characteristic peaks at 2θ = 23.5° and 43.2°, which correspond to diffraction from (002) plane and (101) plane of graphite.

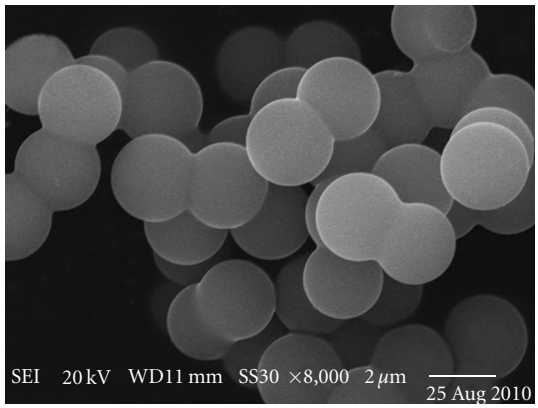

(a)

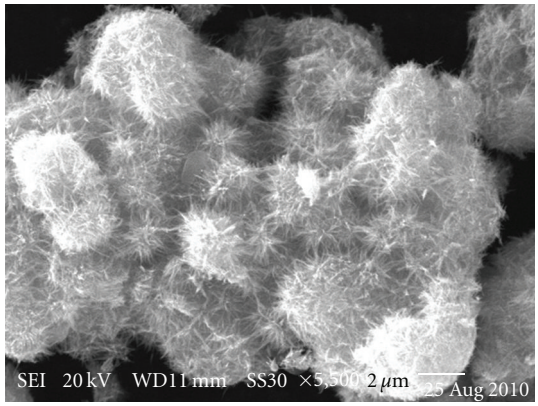

(b)

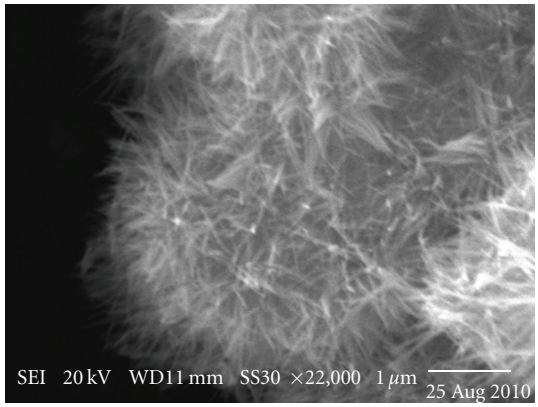

(c)

Figure 1: SEM images of ACMB (a) and γ-MnO_2 nanofibre/ACMB composite (b) low magnification, (c) high magnification.

The broad diffraction peaks suggest a highly disordered and amorphous structure of the ACMB. Simultaneously, the clear appearance of two diffraction peaks indicates that the ACMB is a partial graphitization carbon. Hence, the ACMB has an improved electrical conductivity. Besides two diffraction peaks corresponding to graphite planes of ACMB Figure 2(a), some new diffraction peaks can be observed in Figure 2(b). In Figure 2(b), the diffraction peaks were positioned at $2\theta = 22.1°$, $36.7°$, $42.0°$, $55.7°$, and $65.0°$,

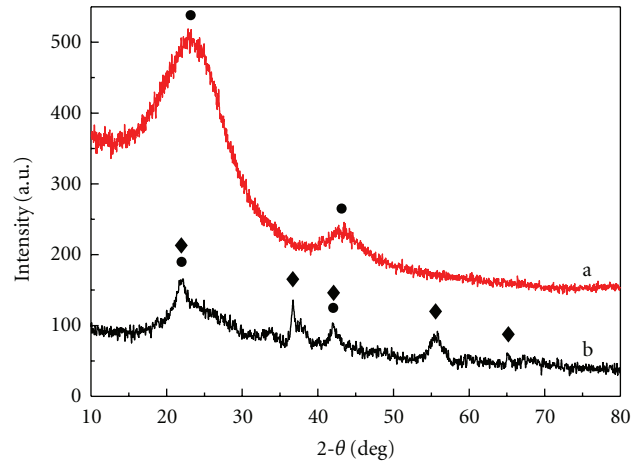

a: ACMB
b: γ-MnO_2 nanofibre/ACMB

Figure 2: XRD patterns of ACMB and γ-MnO_2 nanofibre/ACMB (the peaks of carbon and γ-MnO_2 are noted with (•) and (♦), resp.).

respectively. All characteristic peaks can be indexed to the (110), (201), (211), (221), and (520) planes of orthorhombic γ-MnO_2 (JCPDS card no. 82-2169). Therefore, it can actually be considered that the composite is consisted of ACMB encapsulated by γ-MnO_2 nanofibre.

3.2. Electrochemical Characterization of γ-MnO_2 Nanofibre/ACMB Composite. In order to evaluate the electrochemical characteristics of γ-MnO_2 nanofibre/ACMB composite, cyclic voltammetry and galvanostatic charge/discharge were used to characterize the electrochemical capacitance behavior. Figure 3(a) shows cyclic voltammograms for ACMB electrode and γ-MnO_2 nanofibre/ACMB composite electrode. It can be found that the capacitance characteristic of the ACMB is typically electric double-layer capacitance, which can generally produce a CV curve close to the ideal rectangular shape. By contrast, the CV curve for the γ-MnO_2 nanofibre/ACMB composite electrode showed the presence of significant redox peaks, indicating that faradic reactions took place during the charge/discharge processes. Besides, it can be seen from Figure 3(a) that the area surrounded by CV curve for the γ-MnO_2 nanofibre/ACMB composite electrode is apparently more than one of the ACMB electrode, indicating that the γ-MnO_2 nanofibre/ACMB electrode has much more specific capacitance than ACMB. The difference of CV curves for ACMB and γ-MnO_2 nanofibre/ACMB composite is attributed to the different capacitance mechanisms. The pure ACMB showed an electrical double-layer capacitance, whereas the γ-MnO_2 nanofibre/ACMB composite possessed a combination of both electrical double-layer capacitance and pseudocapacitance.

For CV measurement, the specific capacitances of electrode can be estimated based on the following equation [20]:

$$C = \frac{Q}{V} = \int \frac{idt}{\Delta V}, \quad (1)$$

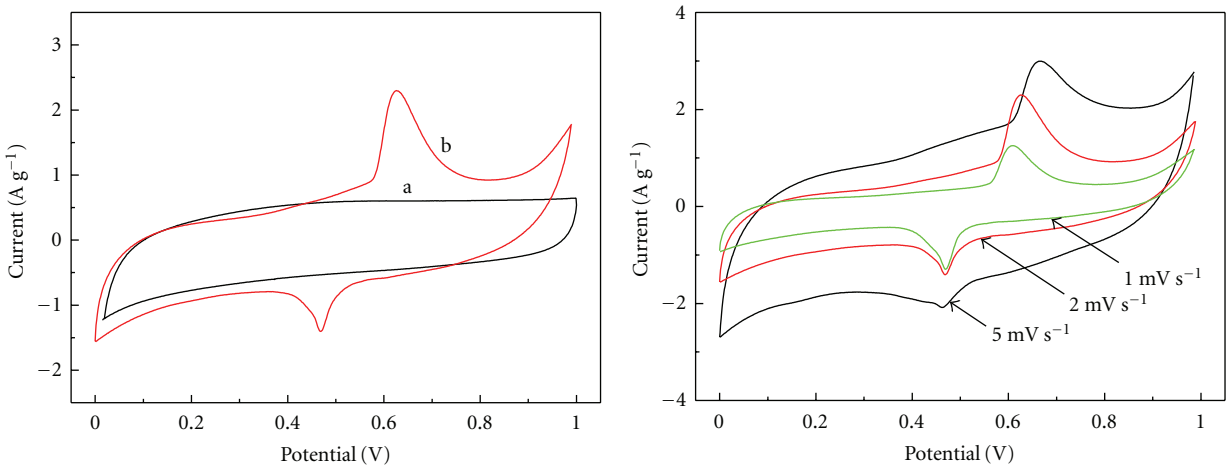

FIGURE 3: Cyclic voltammograms of (a) ACMB and γ-MnO_2 nanofibre/ACMB composite at a scan rate of 2 mV s^{-1} and (b) γ-MnO_2 nanofibre/ACMB composite at different scan rates.

where i is a sampled current, dt is a sampling time span, and ΔV is the total potential deviation of the voltage window.

Figure 3(b) shows cyclic voltammograms of the γ-MnO_2 nanofibre/ACMB electrode at different scan rates. The specific capacitances of ACMB and γ-MnO_2 nanofibre/ACMB are tabulated in Table 1. It can be found from Table 1 that the specific capacitance of the γ-MnO_2 nanofibre/ACMB electrodes is obviously higher than that of ACMB at every given scan rate. The reason is probably that the capacitance of the γ-MnO_2 nanofibre/ACMB electrodes is combination of double-layer capacitance (ACMB) and faradic pseudocapacitance (γ-MnO_2). In addition, it can also be seen from Figure 3(b) that the redox current of γ-MnO_2 nanofibre/ACMB electrode increases clearly with the increasing of the scan rate, indicating its good rate ability.

In order to gain a further understanding on the electrochemical performance of γ-MnO_2 nanofibre/ACMB composite material, the comparison of galvanostatic charge/discharge curves for the ACMB electrode and γ-MnO_2 nanofibre/ACMB composite electrode at 0.5 A g^{-1} is shown in Figure 4(a). The charge/discharge curve of ACMB is almost linear, which indicates that ACMB has good electrical double-layer properties. In comparison, the charge/discharge curve of γ-MnO_2 nanofibre/ACMB composite electrode deviates from ideal linear, and it can be attributed to different capacitive behavior of γ-MnO_2 nanofibre/ACMB electrode. Besides, the charge/discharge curve of γ-MnO_2 nanofibre/ACMB exhibits longer charge/discharge duration than one of the ACMB, indicating an enhancing charge storage capacity, which is mainly ascribed to faradic capacitance of γ-MnO_2.

The charge/discharge curves of the γ-MnO_2 nanofibre/ACMB composite electrodes at different current densities are shown in Figure 4(b). As being seen from Figure 4(b), the discharge time of γ-MnO_2 nanofibre/ACMB composite electrode quickly drops as the current density increases. It may be because at the low current density, the ions have enough time to diffuse into the micropore of γ-MnO_2 nanofibre/ACMB; while at the high current density, the ions can only partially penetrate into the micropore of active material. The specific capacitance of supercapacitor can be evaluated from the charge/discharge test according to the following equation [21]:

$$C = \frac{I \cdot \Delta t}{\Delta V \cdot m}, \tag{2}$$

where I, Δt, ΔV, and m were the current used for charge/discharge, A, the time elapsed for the charge or discharge cycle, s, the voltage interval of the charge or discharge, V, and the mass of activated carbon on the electrodes, g, respectively.

In order to gain a further understanding on the electrochemical performance of γ-MnO_2 nanofibre/ACMB composite material, ACMB and γ-MnO_2 nanofibre/ACMB was used as electrode-active materials of symmetrical supercapacitor, respectively. The variation of specific capacitances of the ACMB and γ-MnO_2 nanofibre/ACMB supercapacitor during 1000 cycles is shown in Figure 5. A significant improvement of the specific capacitance occurs before 200 cycles for the ACMB supercapacitor, which is mainly attributed to a gradual activation process of the active material ACMB. After 200 consecutive cycles, the capacitance of the ACMB supercapacitor was fixed at a steady value. However, it has been seen that the supercapacitor with γ-MnO_2 nanofibre/ACMB possesses markedly much higher specific capacitance than with ACMB. Furthermore, the specific capacitance of the supercapacitor with γ-MnO_2

Table 1: Specific capacitance (F g^{-1}) of ACMB and γ-MnO_2 nanofibre/ACMB at different scan rates·

	10 mV s^{-1}	5 mV s^{-1}	2 mV s^{-1}	1 mV s^{-1}
ACMB	148.6	186.5	238.1	266.3
γ-MnO_2 nanofibre/ACMB	232.6	261.7	330.1	375.9

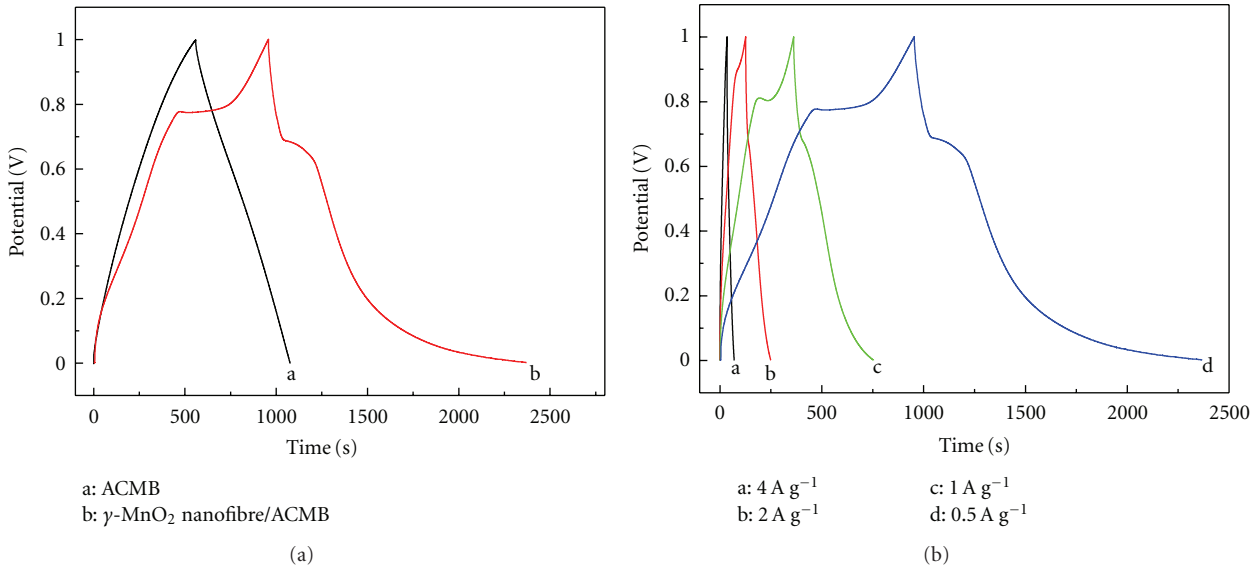

Figure 4: Charge/discharge curves of (a) ACMB and γ-MnO_2 nanofibre/ACMB composite at a current density of 0.5 A g^{-1} and (b) γ-MnO_2 nanofibre/ACMB electrode at different current densities.

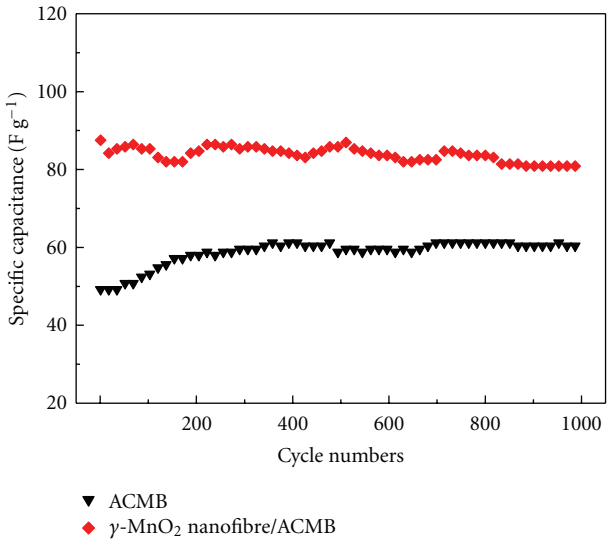

Figure 5: Cycle life curves of ACMB and γ-MnO_2 nanofibre/ACMB supercapacitors at a current density of 0.5 A g^{-1}.

nanofibre/ACMB displays excellent cyclic stability and only 7% decay after 1000 consecutive cycles. Therefore, the γ-MnO_2 nanofibre/ACMB can be considered as a promising electrode-active material for long-term supercapacitor applications.

4. Conclusions

Dandelion-like γ-MnO_2 nanofibre/ACMB composite was successfully prepared by an in situ coating process on the surface of ACMB. Dandelion-like γ-MnO_2 nanofibre/ACMB composite for the application of supercapacitor showed excellent electrochemical performances. The specific capacitance of the supercapacitor using γ-MnO_2 nanofibre/ACMB as electrode-active material is apparently higher than one of the supercapacitor using ACMB as electrode-active material because the specific capacitance of the γ-MnO_2 nanofibre/ACMB is combination of double-layer capacitance (ACMB) and faradic pseudocapacitance (γ-MnO_2). The specific capacitance of the γ-MnO_2 nanofibre/ACMB composite electrode calculated from CV curve is as high as 375.9 F g^{-1} at 1 mV s^{-1}, which is significantly higher than that of ACMB electrode (266.3 F g^{-1}). Besides, the capacitance retention of the supercapacitor with γ-MnO_2 nanofibre/ACMB composite as electrode-active material is up to 93% after 1000 cycles. Therefore, it is obviously proved that the γ-MnO_2 nanofibre/ACMB composite exhibits extensive potential as high-efficiency electrode material of supercapacitor.

Acknowledgments

This work was financially supported by the National Natural Science Foundation of China (Grants Nos. 51072173 and 20871101) and Doctoral Fund of Ministry of Education of China (Grant No. 20094301110005).

References

[1] O. Ghodbane, J.-L. Pascal, and F. Favier, "Microstructural effects on charge storage properties in MnO_2 based electrochemical supercapacitors," *Applied Materials interfaces*, vol. 5, pp. 1130–1139, 2009.

[2] B. E. Conway, *Electrochemical Supercapacitors: Scientific Fundamental and Technological Applications*, Plenum Press, New York, NY, USA, 1999.

[3] A. G. Pandolfo and A. F. Hollenkamp, "Carbon properties and their role in supercapacitors," *Journal of Power Sources*, vol. 157, no. 1, pp. 11–27, 2006.

[4] C. Peng, S. Zhang, D. Jewell, and G. Z. Chen, "Carbon nanotube and conducting polymer composites for supercapacitors," *Progress in Natural Science*, vol. 18, no. 7, pp. 777–788, 2008.

[5] J. Li, X. Wang, Q. Huang, S. Gamboa, and P. J. Sebastian, "A new type of $MnO_2 \cdot xH_2O$/CRF composite electrode for supercapacitors," *Journal of Power Sources*, vol. 160, no. 2, pp. 1501–1505, 2006.

[6] Q. Huang, X. Wang, J. Li, C. Dai, S. Gamboa, and P. J. Sebastian, "Nickel hydroxide/activated carbon composite electrodes for electrochemical capacitors," *Journal of Power Sources*, vol. 164, no. 1, pp. 425–429, 2007.

[7] P. L. Taberna, G. Chevallier, P. Simon, D. Plée, and T. Aubert, "Activated carbon-carbon nanotube composite porous film for supercapacitor applications," *Materials Research Bulletin*, vol. 41, no. 3, pp. 478–484, 2006.

[8] J. Wen and Z. Zhou, "Pseudocapacitance characterization of hydrous ruthenium oxide prepared via cyclic voltammetric deposition," *Materials Chemistry and Physics*, vol. 98, no. 2-3, pp. 442–446, 2006.

[9] C. C. Hu, K. H. Chang, M. C. Lin, and Y. T. Wu, "Design and tailoring of the nanotubular arrayed architecture of hydrous RuO2 for next generation supercapacitors," *Nano Letters*, vol. 6, no. 12, pp. 2690–2695, 2006.

[10] J. P. Zheng, P. J. Cygan, and T. R. Jow, "Hydrous ruthenium oxide as an electrode material for electrochemical capacitors," *Journal of the Electrochemical Society*, vol. 142, no. 8, pp. 2699–2703, 1995.

[11] M. Toupin, T. Brousse, and D. Bélanger, "Charge storage mechanism of MnO_2 electrode used in aqueous electrochemical capacitor," *Chemistry of Materials*, vol. 16, no. 16, pp. 3184–3190, 2004.

[12] H. Kim and B. N. Popov, "Synthesis and characterization of MnO_2-based mixed oxides as supercapacitors," *Journal of the Electrochemical Society*, vol. 150, no. 3, pp. D56–D62, 2003.

[13] C. Lin, J. A. Ritter, and B. N. Popov, "Characterization of sol-gel-derived cobalt oxide xerogels as electrochemical capacitors," *Journal of the Electrochemical Society*, vol. 145, no. 12, pp. 4097–4103, 1998.

[14] H. Wang, Z. Li, J. Yang, Q. Li, and X. Zhong, "A novel activated mesocarbon microbead(aMCMB)/Mn_3O_4 composite for electrochemical capacitors in organic electrolyte," *Journal of Power Sources*, vol. 194, no. 2, pp. 1218–1221, 2009.

[15] V. Srinivasan and J. W. Weidner, "Studies on the capacitance of nickel oxide films: effect of heating temperature and electrolyte concentration," *Journal of the Electrochemical Society*, vol. 147, no. 3, pp. 880–885, 2000.

[16] K. R. Prasad and N. Miura, "Electrochemically deposited nanowhiskers of nickel oxide as a high-power pseudocapacitive electrode," *Applied Physics Letters*, vol. 85, no. 18, pp. 4199–4201, 2004.

[17] D. Portehault, S. Cassaignon, E. Baudrin, and J. P. Jolivet, "Design of hierarchical core-corona architectures of layered manganese oxides by aqueous precipitation," *Chemistry of Materials*, vol. 20, no. 19, pp. 6140–6147, 2008.

[18] H. Zhang, G. Cao, Z. Wang, Y. Yang, Z. Shi, and Z. Gu, "Growth of manganese oxide nanoflowers on vertically-aligned carbon nanotube arrays for high-rate electrochemical capacitive energy storage," *Nano Letters*, vol. 8, no. 9, pp. 2664–2668, 2008.

[19] G. Lv, D. Wu, and R. Fu, "Preparation and electrochemical characterizations of MnO_2-dispersed carbon aerogel as supercapacitor electrode material," *Journal of Non-Crystalline Solids*, vol. 355, no. 50-51, pp. 2461–2465, 2009.

[20] H. An, Y. Wang, X. Wang et al., "Polypyrrole/carbon aerogel composite materials for supercapacitor," *Journal of Power Sources*, vol. 195, no. 19, pp. 6964–6969, 2010.

[21] Y. G. Wang, H. Q. Li, and Y. Y. Xia, "Ordered whiskerlike polyaniline grown on the surface of mesoporous carbon and its electrochemical capacitance performance," *Advanced Materials*, vol. 18, no. 19, pp. 2619–2623, 2006.